

Epsilon-Unfolding Orthogonal Polyhedra

Mirela Damian*

Robin Flatland†

Joseph O'Rourke‡

Abstract

An *unfolding* of a polyhedron is produced by cutting the surface and flattening to a single, connected, planar piece without overlap (except possibly at boundary points). It is a long unsolved problem to determine whether every polyhedron may be unfolded. Here we prove, via an algorithm, that every *orthogonal polyhedron* (one whose faces meet at right angles) of genus zero may be unfolded. Our cuts are not necessarily along edges of the polyhedron, but they are always parallel to polyhedron edges. For a polyhedron of n vertices, portions of the unfolding will be rectangular strips which, in the worst case, may need to be as thin as $\epsilon = 1/2^{\Omega(n)}$.

1 Introduction

Two unfolding problems have remained unsolved for many years [DO05]: (1) Can every convex polyhedron be edge-unfolded? (2) Can every polyhedron be unfolded? An *unfolding* of a 3D object is an isometric mapping of its surface to a single, connected planar piece, the “net” for the object, that avoids overlap. An *edge-unfolding* achieves the unfolding by cutting edges of a polyhedron, whereas a *general unfolding* places no restriction on the cuts. General unfoldings are known for convex polyhedra, but not for nonconvex polyhedra. It is known that some nonconvex polyhedra cannot be edge-unfolded, but no example is known of a nonconvex polyhedron that cannot be unfolded with unrestricted cuts. The main result of this paper is that the class of genus-zero orthogonal polyhedron have a general unfolding. As we only concern ourselves with general unfoldings of genus-zero polyhedra in this paper, we will drop the “general” and “genus-zero” modifiers when clear from the context.

The difficulty of the unfolding problem has led to a focus on *orthogonal polyhedra*—those whose faces meet at angles that are multiples of 90° —and especially on genus-zero polyhedra, i.e., those whose surface is homeomorphic to a sphere. This line of investigation was initiated in [BDD⁺98], which established that certain subclasses of orthogonal polyhedra have an unfolding: *orthostacks* and *orthotubes*. Orthostacks are extruded orthogonal polygons stacked along one coordinate direction. The orthostack algorithm does not achieve an edge unfolding, but it is close, in a sense we now describe.

A *grid unfolding* adds edges to the surface by intersecting the polyhedron with planes parallel to Cartesian coordinate planes through every vertex. This concept has been used to achieve grid *vertex unfoldings* of orthostacks [DIL04], and later, grid vertex unfoldings of all genus-zero orthogonal polyhedra [DFO06]. (A “vertex unfolding” is a loosening of the notion of unfolding that we do not pause to define [DEE⁺03].) A $k_1 \times k_2$ *refinement* of a surface [DO04] partitions each face further into a $k_1 \times k_2$ grid of faces; thus a 1×1 refinement is an unrefined grid unfolding. The orthostack

*Dept. Comput. Sci., Villanova Univ., Villanova, PA 19085, USA. mirela.damian@villanova.edu.

†Dept. Comput. Sci., Siena College, Loudonville, NY 12211, USA. flatland@siena.edu.

‡Dept. Comput. Sci., Smith College, Northampton, MA 01063, USA. orourke@cs.smith.edu. Supported by NSF Distinguished Teaching Scholars award DUE-0123154.

algorithm achieves a 2×1 refined grid unfolding. It remains open to achieve a grid unfolding of orthostacks. (It is known that not all orthostacks may be edge unfolded.)

The algorithm we present in this paper could be characterized as achieving a $2^{O(n)} \times 2^{O(n)}$ refined grid unfolding of orthogonal polyhedra of n vertices. We coin the term *epsilon-unfolding* to indicate a refinement with no constant upper bound, but which instead grows with n . In our case, some portions of the unfolding might be ϵ -thin, with $\epsilon = 1/2^{\Omega(n)}$.

Our algorithm has its roots in the staircase unfolding of [BDD⁺98], in the spiral strips used in [DFO05], and the band structure exploited in [DFO06], but introduces several new ideas, most notably a recursive spiraling pattern whose nesting leads to the ϵ -thin characteristic of the unfolding.

1.1 Definitions

Let O be a solid, genus-zero, orthogonal polyhedron. We assume O has all edges parallel to xyz axes of a Cartesian coordinate system. We use the following notation to describe the six types of faces of O , depending on the direction in which the outward normal points: *front*: $-y$; *back*: $+y$; *left*: $-x$; *right*: $+x$; *bottom*: $-z$; *top*: $+z$. We take the z -axis to define the vertical direction. The spiral paths that play a key role in our algorithm will wrap around top, right, bottom, left faces, and “move” in the front/back y -direction.

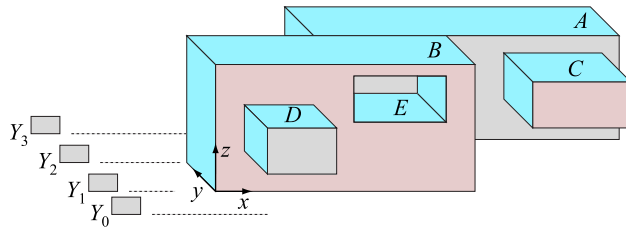


Figure 1: Definitions: A , B , C , and D are protrusions; E is a dent.

Let Y_i be the plane $y = y_i$ orthogonal to the y -axis. Let $Y_0, Y_1, \dots, Y_i, \dots$ be a finite sequence of parallel planes passing through every vertex of O , with $y_0 < y_1 < \dots < y_i < \dots$. We call the portion of O between planes Y_i and Y_{i+1} *layer i* ; it includes a collection of disjoint connected components of O . We call each such component a *slab*. Referring to Figure 1, layer 0, and 2 each contain one slab (D and A , respectively), whereas layer 1 contains two slabs (B and C). The surface piece that surrounds a slab is called a *band* (labeled in Figure 1). Each band has two *rims*, the cycle of edges that lie in its bounding Y_i and Y_{i+1} planes. Each slab is bounded by an outer band, but it may also contain inner bands, bounding holes. Outer bands are called *protrusions* and inner bands are called *dents* (E in Figure 1).

1.2 Dents vs. Protrusions

As we observed in [DFO06], dents may be treated exactly the same as protrusions with respect to unfolding, because unfolding of a 2-manifold to another surface (in our case, a plane) depends only on the intrinsic geometry of the surface, and not on how it is embedded in \mathbb{R}^3 . Note that we are only concerned with the final unfolded “flat state” [DO05], and not about possible intersections during a continuous sequence of partially unfolded intermediate states. All that matters for unfolding is which faces share an edge, and the cyclic ordering of the faces incident to a vertex, i.e., our unfolding algorithms will make local decisions and will be oblivious to the embedding in \mathbb{R}^3 . These local relationships are identical if we conceptually “pop-out” dents to become protrusions (this

popping-out is conceptual only, for it could produce self-intersecting objects.) Henceforth, we will describe only protrusions in our algorithms, with the understanding that nothing changes for dents. This shows that our algorithm works on a wider class of objects than the orthogonal polyhedra, an observation we do not pursue.

1.3 Overview

The algorithm first partitions the polyhedron O by the Y_i planes, and then forms an “unfolding tree” T_U whose nodes are bands, and with a parent-child arc representing a “z-beam” of visibility in their shared Y_i plane that connects the bands. “Front-” and “back-child” arcs are distinguished according to the relative y -positions of the children with respect to the parent. The recursion follows a preorder traversal of this tree. A thin spiral path winds around the {top, right, bottom, left} faces of a root band b , visits each of the front children recursively, and then each of the back children recursively. The children are visited in a parentheses-nesting order that is forced by the turn-around requirements. At all times the spiral alternates turns so that its unfolding to the plane is a staircase-like path monotone with respect to the horizontal. (Cf. Figures 3, 4, 14, 19.) When the path finishes spiraling around the last back child of b , it is deeply nested inside the spiral, and must retrace the entire path to return adjacent to its starting point. (It is this retracing, recursively encountered, that causes the exponential thinness.) Again this is accomplished while maintaining the staircase-like layout. Finally, the front and back faces are hung above and below the staircase. Following the physical model of cutting out the net from a sheet of paper, we permit cuts representing *edge overlap*, where the boundary touches but no interior points overlap. This can occur when hanging the front and back faces (cf. Figures 14, 19).

2 Unfolding Extrusions

It turns out that nearly all algorithmic issues are present in unfolding polyhedra that are extrusions of simple orthogonal polygons. Therefore we will describe the algorithm for this simple shape class first, in detail, and then show that the ideas extend directly to unfolding all orthogonal polyhedra.

Let O be a polyhedron that is an extrusion in the z direction of a simple orthogonal polygon. We start with the partition π of O induced by the Y_i planes passing through every vertex, as described in Section 1. Each element in the partition is a band with exactly four faces encompassing a rectangular box. The dual graph of π has a node for each band and an edge between each pair of adjacent bands. For ease of presentation, we will use the terms *node* and *band* interchangeably. Because O is simply connected, the dual graph is a tree T_U , which we refer to as the *unfolding tree*. The root of T_U is any band that intersects Y_0 . See Figure 2.

We distinguish between the two rims of each band via a recursive classification scheme. The rim of the root band at y_0 is the *front* rim; the other one is the *back* rim. For any other band b , the rim of b adjacent to the parent of b is the *front* rim, and the other is the *back* rim. In Figure 2a, for example, the front rim of b_8 is at y_1 . A child is a *front child* (*back child*) if it is adjacent to the front (back) rim of its parent. In Figure 2b, thin arcs connect a parent to its front children; thick arcs connect a parent to its back children.

In the following we describe the recursive unfolding algorithm. We begin by establishing that there exists a simple spiraling path ξ on the surface of O that starts and ends on the front rim of the root band and winds around each band in T_U at least once. When this path is “thickened”, it covers the band faces and unfolds into a horizontal staircase-like strip to which front and back faces of O can be attached vertically. We describe ξ recursively, starting with the base case in which O consists of a single box and thus the partition π leaves a single band.

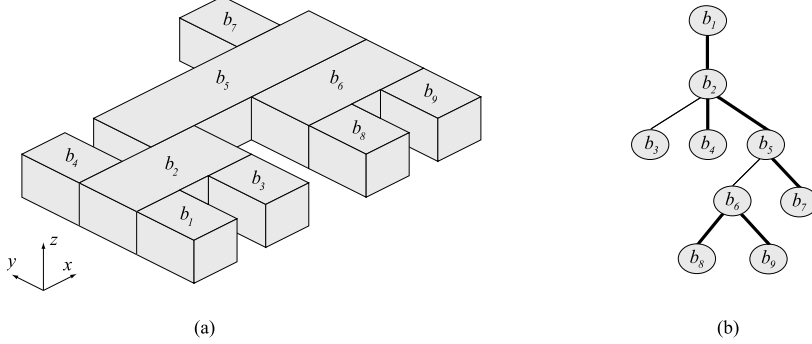


Figure 2: (a) Partition of O 's x and z perpendicular faces into bands. (b) Unfolding tree T_U . Thin arcs connect a parent to its front children; thick arcs connect it to its back children.

2.1 Single Box Spiral Path

Let O be a box with band b . We use the following notation (see Figure 3a): A , B , C , and D are top, right, bottom and left faces of O (these faces belong to b); E and F are back and front faces of O (these faces do not belong to b); s and t are *entering* and *exiting* points on the top edge of the front rim of b .

The main idea is to start at s , spiral forward (front to back, cw or ccw) around band faces A , B , C and D , cross the back face E to reverse the direction of the spiral, then spiral backward (back to front, ccw or cw) around band faces back to t . See Figure 3a for an example, where mirror views are provided for the bottom, left, and back faces which cannot be viewed directly. We refer to the forward spiral (incident to entering point s) as the *entering* spiral, and the backward spiral (incident to exiting point t) as the *exiting* spiral. Spiral ξ is the concatenation of the entering spiral, the back face strip, and the exiting spiral. It can be unfolded flat and laid out horizontally in a plane, as illustrated in Figure 3b.

We distinguish four variations of this spiraling path, which differ in how they enter and exit the band: the entering spiral is heading away from s either to the right (cw) or to the left (ccw), and t is either to the left or to the right of s on the front edge. Directions left, right, cw, and ccw are defined from the perspective of a viewer positioned at $y = -\infty$. We will use the notation R_{st} , R_{ts} , L_{st} and L_{ts} , to identify the four possible entering/exiting configurations. Here the first letter (R or L) indicates the direction (Right or Left) the entering spiral is heading as it moves away from s , and the subscripts indicate the position of s relative to t . We use the symbol R_- for b to indicate that the relative position of s and t is irrelevant to this discussion; thus R_- denotes either R_{st} or R_{ts} , and same for L_- . For the base case, Figures 3a, 4a, 5a and 5b illustrate all four configurations R_{st} , R_{ts} , L_{ts} and L_{st} , respectively. The unfoldings for all four cases are similar, each flattening into a horizontal staircase-like strip.

Three dimensional illustrations of ξ , such as the ones in Figures 3a and 4a, are impractical for all but the smallest examples. To be able to illustrate more complex unfoldings, we define a simple 2D representation for each of the base case variations of ξ , as in Fig. 6. Note that each 2D representation captures critical information that defines the spiral path: the direction (R or L) of the entering spiral, and the relative position of s and t . The entrance is connected in a loop to the exit: the turnaround arc corresponds to the forward spiral reversing its direction (cw to ccw, or ccw to cw) using a back face strip (strip labeled K_0 in Figures 3a, 4a, 5).

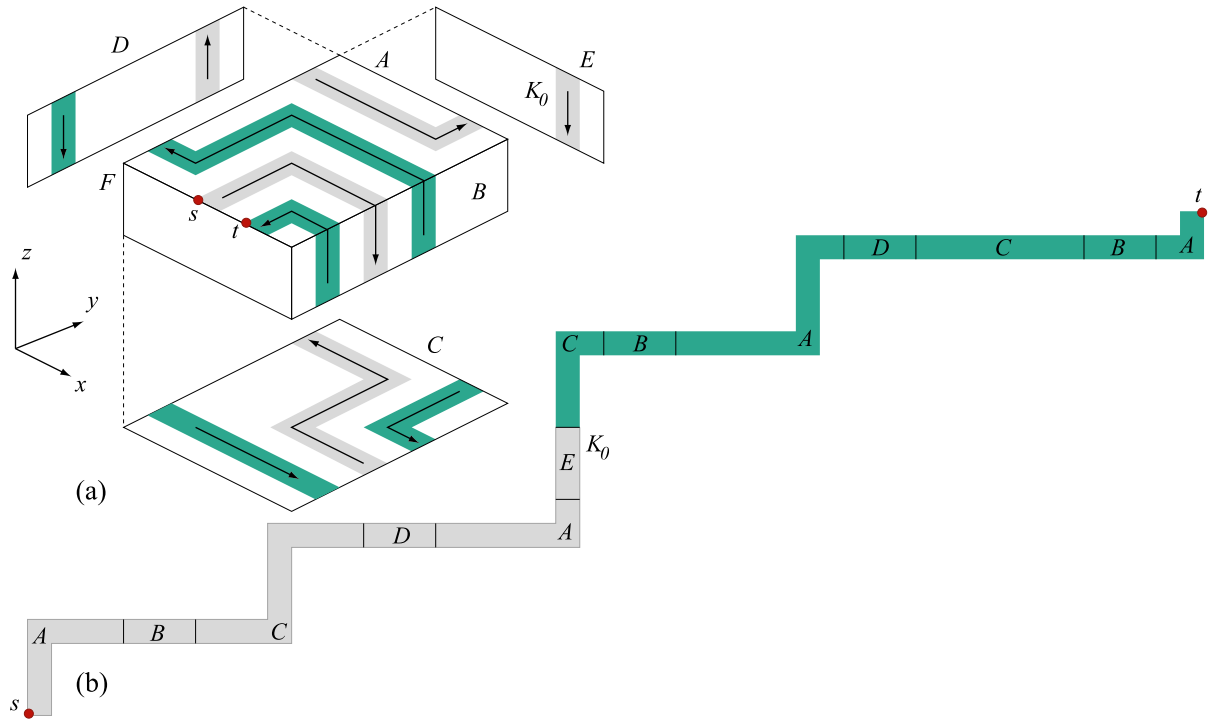


Figure 3: (a) Spiral path ξ with entering/exiting configuration R_{st} : s is left to t , and entering spiral heads rightward from s . (b) Flattened spiral ξ .

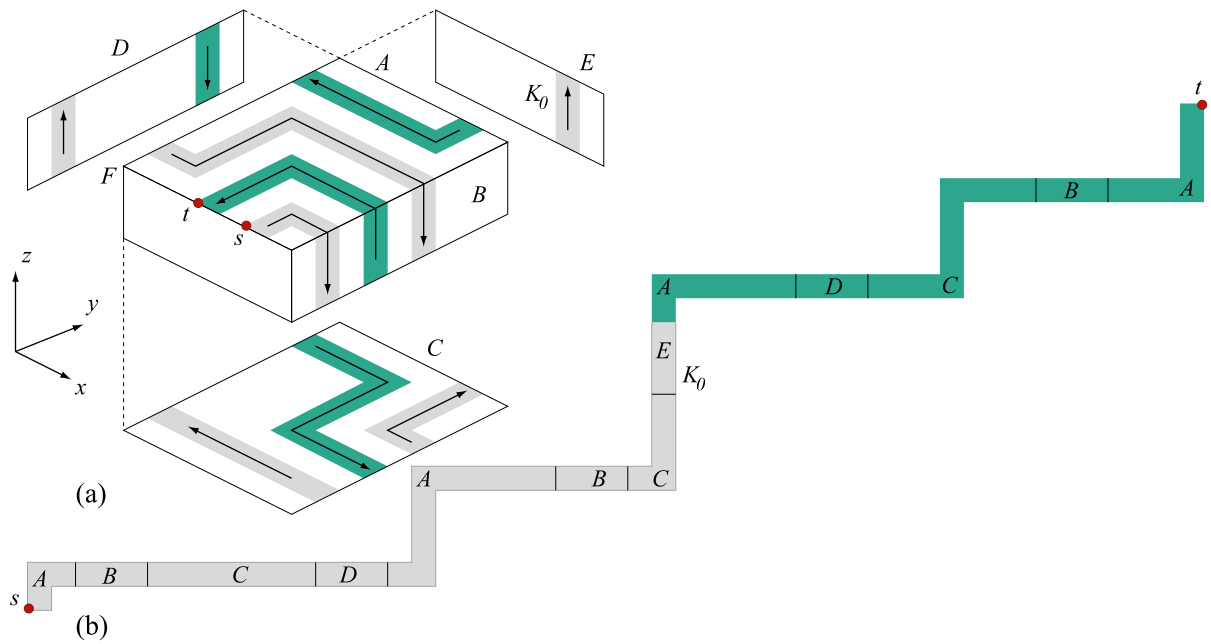


Figure 4: (a) Spiral path ξ with entering/exit configuration R_{ts} : s right of t ; entering spiral heads right from s . (b) Flattened spiral ξ .

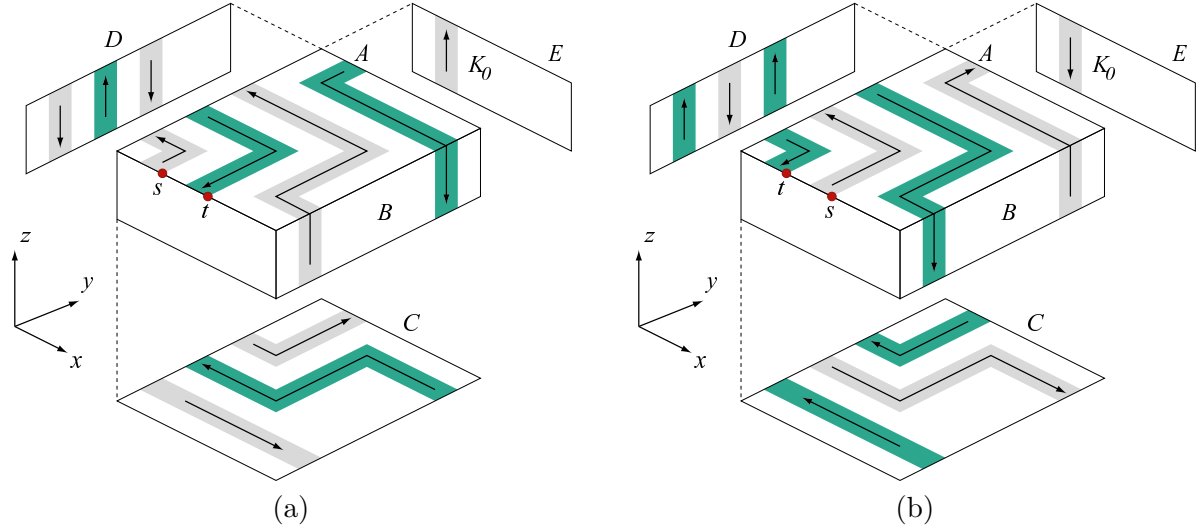


Figure 5: (a) Spiral path ξ with entering/exiting configuration L_{st} : s is left of t , and entering spiral heads left from s . (b) Spiral path ξ with entering/exiting configuration L_{ts} : s is right of t , and entering spiral heads left from s .

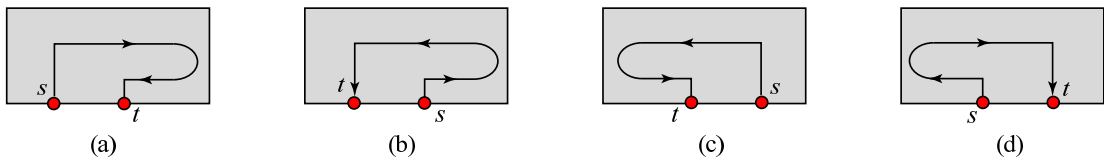


Figure 6: 2D representations of four base case variations of ξ illustrating entering/exiting configurations (a) R_{st} (b) R_{ts} (c) L_{ts} (d) L_{st} .

2.2 Recursive Structure

In general, a band b has children adjacent along its front and back rims. The spiral path ξ for the subtree rooted at b begins and ends at two proximate points s and t on the top edge of b 's front rim. The entering and exiting spirals of b conform to one of the four entering/exiting configurations R_{st} , R_{ts} , L_{st} or L_{ts} .

We describe ξ at a high level first. Once b 's entering spiral leaves s , it follows an alternating path to reach each of the front children of b and spiral around them recursively. An alternating path is required because after spiraling around a child of b , the direction of b 's spiral is reversed. After visiting the front children, b 's entering spiral cycles forward around b to its back rim, where it follows a second alternating path to reach each of the back children and spiral around them recursively. After visiting the last back child, b 's exiting spiral returns to t , tracking the path taken by the entering spiral, but in reverse direction. This final reverse spiral will revisit nodes/boxes already visited on the forward pass, and the recursive structure will imply that some nodes/boxes will be revisited many times before the spiral returns to t . We defer discussion of this consequence of the algorithm to Section 4.

2.2.1 Alternating Paths for Labeling Children

A preorder traversal of T_U assigns each band an entering/exiting configuration label (R_{st} , R_{ts} , L_{st} , or L_{ts}). Although any label would serve for the root box of T_U , for definitiveness we label it R_{ts} . We also pick an entering and an exiting point on top of the root's front rim, with the exiting point to the left of the entering point, which is consistent with its R_{ts} label. In the following we provide rules for labeling the front and back children of a labeled parent b , which get applied when b is visited during the traversal. These rules are described in terms of two alternating paths that b 's entering spiral takes to reach every front and back child. We begin with the alternating path for labeling the front children.

LABEL-FRONT-CHILDREN(b) (see Figure 7)

1. Set current position to s . Set current direction to the direction of the entering spiral of b : rightward, if b has an R -label, and leftward if an L -label.
2. **while** b has unlabeled front children **do**
 - (a) From the current position, walk in the current direction along the front rim of b , until
 - (i) an unlabeled front child b_i is encountered, and (ii) current position is on top of b .
 - (b) Assign to b_i label R_{st} if walking rightward, or L_{ts} if walking leftward. Select points s_i and t_i on the top line segment at the intersection between b and b_i , in a relative position consistent with the label (R_{st} or L_{ts}) of b_i . Reverse the current direction.

We must reverse the current direction in Step (b) above because the spiral exits a child box heading in the opposite direction from which it entered: if the entering spiral heads rightward, the exiting spiral heads leftwards, and the other way around. This forces the left/right alternation between the front children of b . Figure 7 shows an example in which b has five front children and an R -type configuration. The children are visited in the order b_1, b_2, b_3, b_4 and b_5 ; the dashed lines correspond to walking around side and bottom faces of b , to reach an unlabeled child from the top of b . The configuration assigned to each child by the labeling procedure above is shown within parentheses.

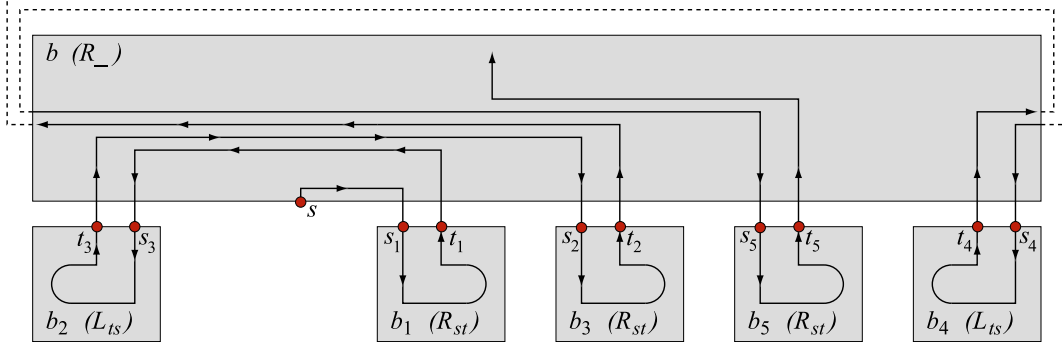


Figure 7: Labeling front children.

After labeling all front children of b , its back children are labeled using a similar scheme. Unlike the situation for front children, however, we have the flexibility of selecting which back child to label first. For definitiveness, we always label first either the leftmost or the rightmost back child, depending on whether the alternating path heads leftward or rightward after labeling the last front child. The procedure below describes the alternating path used to label the back children.

LABEL-BACK-CHILDREN(b) (see Figure 8)

1. Set current position to s , if b has no front children; otherwise, set current position to the exiting point of the front child last labeled.
2. Set current direction to the direction of b 's entering spiral, if b has no front children; otherwise, set current direction to the direction of the exiting spiral of the front child of b last labeled (i.e, leftward, if the child has an R -label, and rightward if it has an L -label).
3. **while** b has unlabeled back children **do**
 - (a) If the current direction is leftward (rightward), then walk leftward (rightward) from the current position, until the leftmost (rightmost) unlabeled back child b_i is encountered.
 - (b) If b_i is not the last unlabeled back child, then assign to b_i label L_{st} (R_{ts}), if the current direction is leftward (rightward).
 - (c) If b_i is the last unlabeled back child, assign to b_i a label with the same ordering of s and t as for b . Specifically, if b has a $_st$ label and b_i is entered while heading leftward (rightward), assign to b_i label L_{st} (R_{st}); if b has a $_ts$ label and b_i is entered while heading leftward (rightward), assign to b_i label L_{ts} (R_{ts}).
 - (d) Select points s_i and t_i on the top line segment at the intersection between b and b_i , in a relative position consistent with the label of b_i . Reverse the current direction.

Note that the relative position of s_i and t_i in the entering/exiting configuration for the back child last labeled stays consistent with the configuration for the parent. Figure 8 shows an example in which b has five back children, and a $_ts$ unfolding configuration. The back children get visited in the order $b_6, b_7, b_8, b_9, b_{10}$. The unfolding label assigned to each back child is shown within parentheses; observe that the unfolding label $_ts$ for b_{10} (the back child last labeled) is consistent with the unfolding label $_ts$ of its parent. Also observe that the nesting of the L/R alternation is inside-out for front children, and outside-in for back children (cf. Figures 7 and 8).

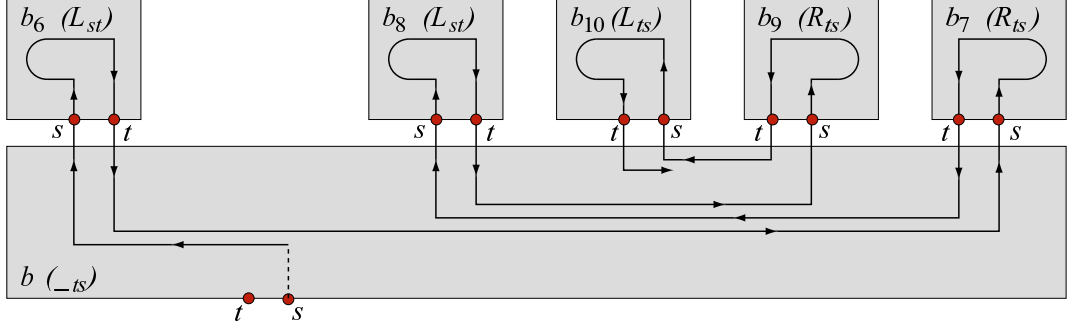


Figure 8: Labeling back children.

The path exiting b_{10} must now return to the exiting point t of parent b , and to do so, because it is deeply nested in the alternating paths, it must follow the entire path between the entering point of b and the entering point of b_{10} , but in reverse direction. We return to this in the next section.

2.2.2 Recursive Spiral Paths

Lemma 1 *For any unfolding tree T_U rooted at a node with entering point s and exiting point t , there exists a simple spiral path ξ such that (i) ξ starts at s , cycles around each band in T_U at least once, and returns to t heading in the reverse direction (ii) for each node b in T_U , ξ is consistent with the entering/exiting configuration for b , and (iii) ξ unfolds flat horizontally, with s on the far left and t on the far right.*

Proof: The proof is by induction on the depth of T_U . The base case corresponds to a tree with a single node b (of depth 1), and is established by Figures 3a, 4, 5a, and 5b.

Assume that the lemma holds for any unfolding tree of depth d or less, and consider an unfolding tree T_U of depth $d + 1$ rooted at b . We only discuss the case in which b has an R_{ts} entering/exiting configuration; the other three cases (R_{st} , L_{ts} and L_{st}) are similar.

We begin with the general case when b has both front and back children. Let $b_1, b_2 \dots b_k$ be the front children and $b_{k+1}, b_{k+2} \dots$ be the back children of b , in the order in which they are visited by the labeling procedures from section 2.2.1. The spiral ξ starts at s and follows the front alternating path illustrated in Figure 7 to reach each front child b_i . We apply the inductive hypothesis on b_i to conclude the existence of a spiral path $\xi(b_i)$ from s_i to t_i for the subtree rooted at b_i . From t_i , ξ continues along the front alternating path to the next front child. Figure 9 illustrates the strip segments along the front and back alternating paths used to reach the children of b : ξ_0 is used to get from s to b_1 , ξ_1 from b_1 to b_2 , and so on.

After visiting the last front child b_k , ξ cycles around b once, stopping at the entering point s_{k+1} of b_{k+1} (see spiral segment ξ_5 in Figure 9). This cycle is necessary to ensure that ξ goes around b at least once. From s_{k+1} , spiral $\xi(b_{k+1})$ takes ξ to t_{k+1} , and from there ξ moves along the back alternating path on to the next back child. The portion of ξ from s to the entering point of the back child last visited is b 's entering spiral. In the example of Figure 9, the entering spiral starts at s and ends at s_{10} .

The unfolding of b 's entering spiral is depicted in Figure 10, where each shaded region contains the horizontal unfolding of $\xi(b_i)$ corresponding to the subtree rooted at b_i . Linking the children's spirals together are the strip segments of the alternating paths and the cycle around b .

Once ξ leaves the last back child, it must return to the exiting point t of b , and it does so by tracking the entering spiral of b in the reverse direction. This portion of ξ is b 's exiting spiral. By

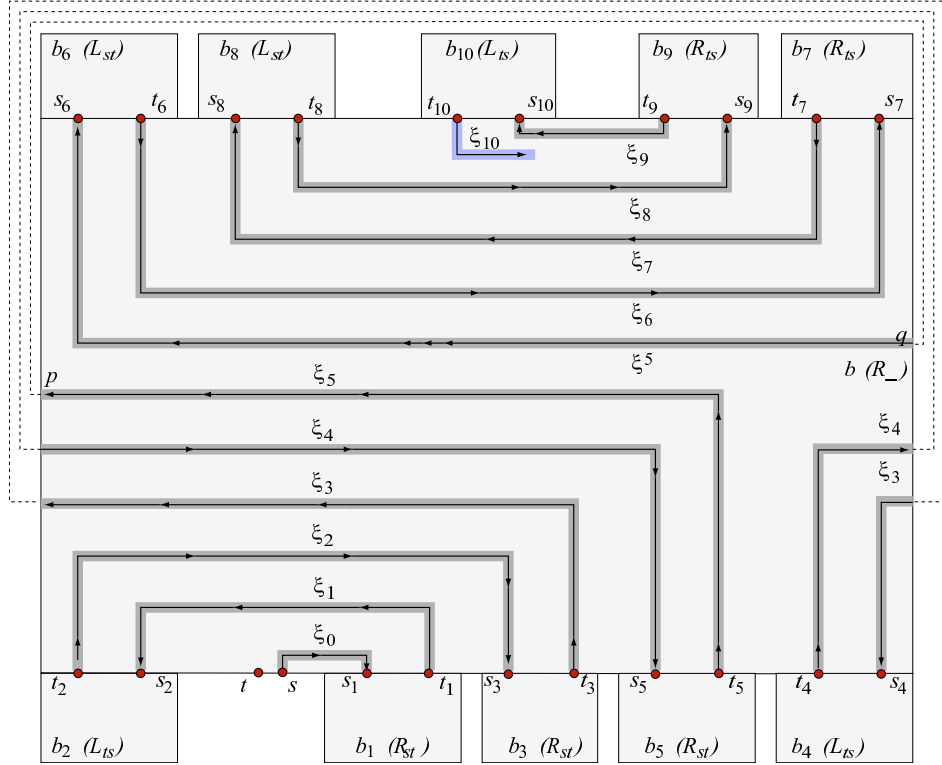


Figure 9: Strip segments along the front and back alternating paths used to reach the children of b : ξ_0 is used to get from s to b_1 , ξ_1 from b_1 to b_2 , and so on.

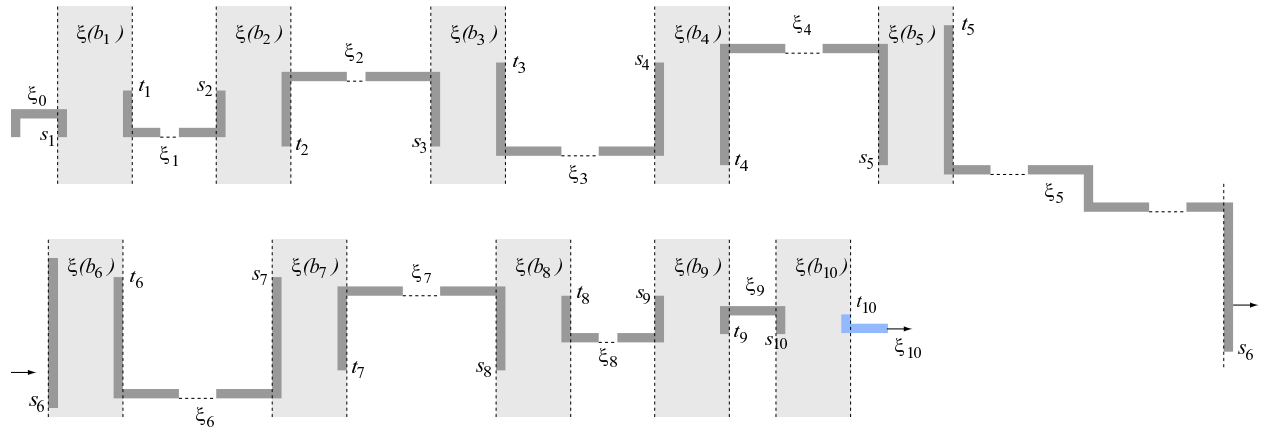


Figure 10: Band b 's entering spiral unfolded.

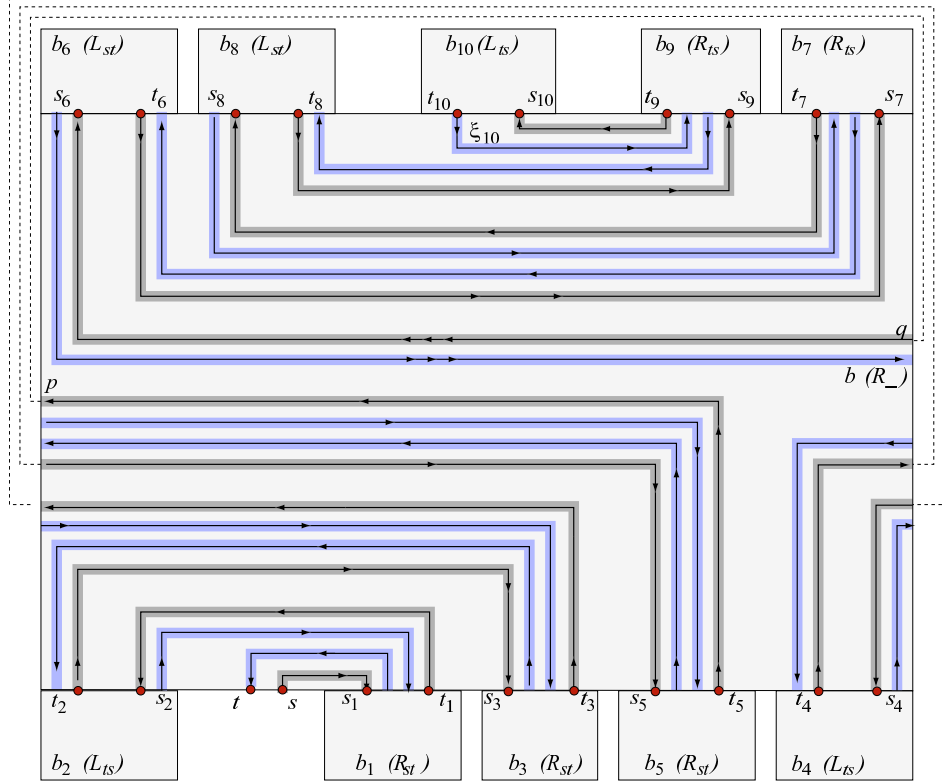


Figure 11: Forward and backward $\xi = \xi(b)$.

making the entering spiral arbitrarily thin and positioning it so that it doesn't touch any edge of O or itself, we ensure that there is room along its sides for the exiting spiral. Figure 11 illustrates all fragments of ξ that belong to b .

As a complete running example, Figure 12 illustrates the spiral ξ in its entirety for the case in which none of the children b_i has children of its own. The spiral for each b_i corresponds to one of the base cases (see Figs. 3, 4 and 5). The entering spiral of b extends from s to s_{10} and visits b_1, b_2, \dots, b_{10} in this order. The exiting spiral of b extends from t_{10} to t and visits $b_9, b_8 \dots b_1$ in this order, tracking closely the entering spiral in reverse.

We now prove that ξ satisfies the three conditions stated in the lemma. It is clear that ξ cycles around each band in T_U at least once: by induction, $\xi(b_i)$ cycles around each band in the subtree rooted at b_i at least once, and ξ cycles around b after visiting the front children. Also note that the exiting spiral ends up at t , left of s . This is because the last visited back child and b have the same $_st$ or $_ts$ label, and b 's exiting spiral tracks its entering spiral in reverse from the last back child's exiting point to t . In Figure 9, the last back child b_{10} has t_{10} to the left of s_{10} , which places b 's entering spiral to the left of its exiting spiral, guaranteeing that the exiting spiral terminates to the left of s . Therefore, ξ satisfies condition (i) of the lemma. By induction, $\xi(b_i)$ is consistent with every configuration in the subtree rooted at b_i , therefore ξ satisfies condition (ii) of the lemma as well.

Figure 10 shows the horizontal unfolding of the entering spiral (from s to s_{10}). The unfolding of the exiting spiral is similar, but rotated 180° . The unfolding of the entire spiral ξ is the concatenation of the unfolded entering spiral, the last back child's spiral, and the exiting spiral. It can be easily verified that this satisfies condition (iii) of the lemma. This completes the proof for the case

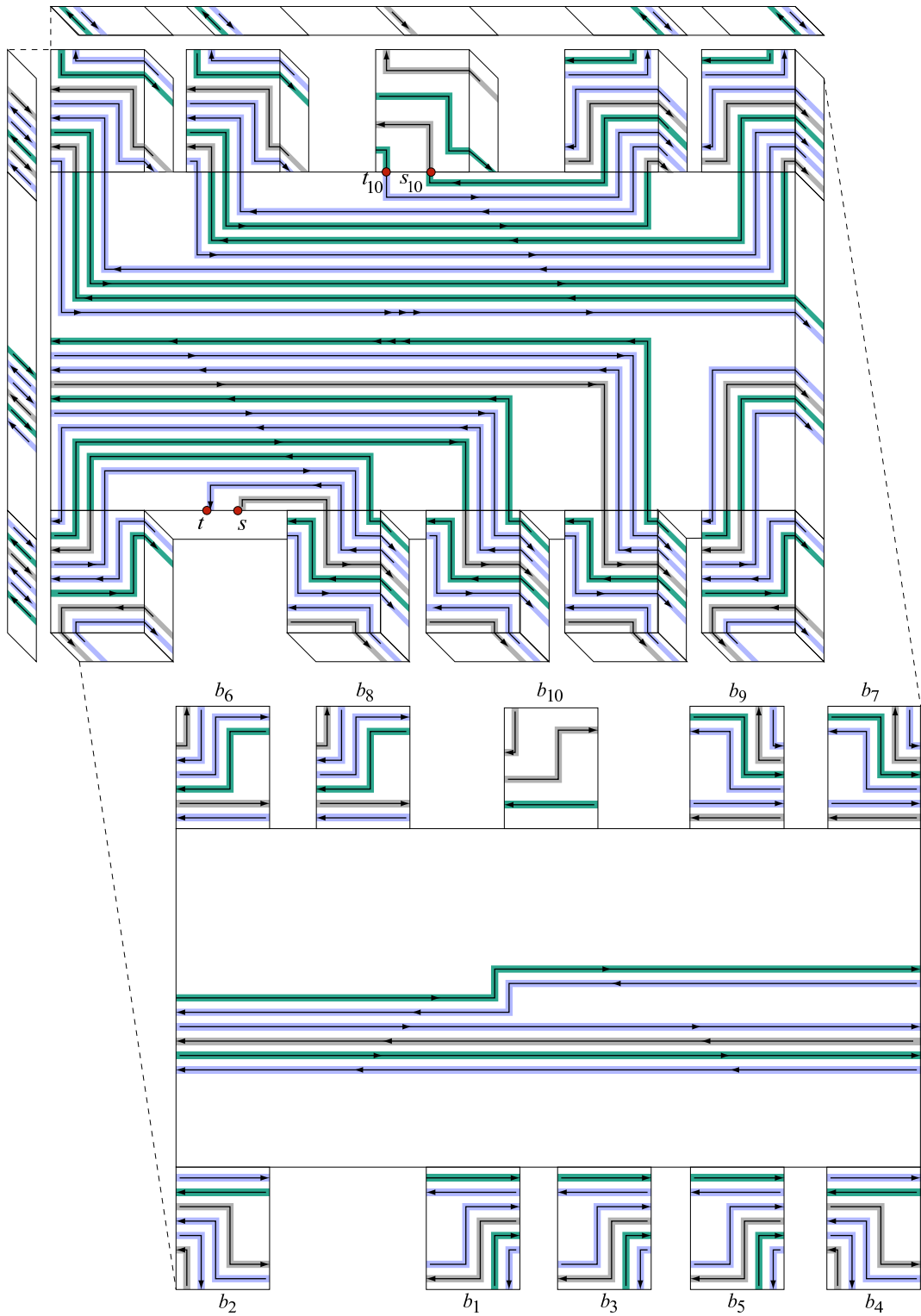


Figure 12: Spiral ξ for a complete example, with mirror views for left, back and bottom faces. Entering spiral for b extends from s to s_{10} and exiting spiral from t_{10} back to t .

when b has front and back children.

If b has no front children, then from s the spiral proceeds to cycling around b and then alternating between the back children. If there are no back children, then after visiting the front children and cycling around b , the spiral reverses its direction using a strip from the back face of b (as done in the base case), then tracks the entering spiral back to t . \square

The proof of Lemma 1 leads to an algorithm for computing the spiral path for a subtree rooted at band b , as described in the procedure SPIRAL-PATH(b) below.

SPIRAL-PATH(b)

1. If b has no front children, skip to Step 3.
2. **while** (b has unvisited front children) **do**
 - 2.1 Follow the front alternating path to the entering point of next front child b_i of b .
 - 2.2 SPIRAL-PATH(b_i).
3. Complete a cycle around b and proceed to the back rim of b .
4. If b has no back children, reverse spiral using a back face strip and skip to Step 6.
5. **while** (b has unvisited back children) **do**
 - 4.1 Follow the back alternating path to the entering point of next back child b_i of b .
 - 4.2 SPIRAL-PATH(b_i).
6. Retrace the entering spiral for b back to the exiting point of b .

2.3 Recursive Spiral Path Example

To reinforce our recursive spiraling ideas, we provide the 2D representation of an unfolding for a slightly more complex example, illustrated in Fig. 13. Observe that the cycle that ξ makes around each band is not captured by a 2D representation, therefore we omit mentioning it in this section.

We first describe the structure of the unfolding tree for our example. Box b_0 is the root of the unfolding tree; it has one back child b_1 and no front children. Box b_1 has two front children, b_2 and b_5 , and two back children, b_7 and b_8 . Box b_2 has two back children, b_3 and b_4 , and no front children. Box b_5 has one front child b_6 and no back children. Box b_8 has two back children, b_9 and b_{10} , and no front children.

The algorithm begins by assigning an R_{ts} label to b_0 , and then uses the procedure from Section 2.2.1 to assign labels to the other boxes, as marked on each box in Fig. 13.

We now discuss the order in which the spiral ξ visits these boxes. From b_0 , ξ enters the back child b_1 and then proceeds along the front alternating path to reach the front child b_2 first. Since b_2 has no front children, ξ proceeds to the back of b_2 to visit its back children b_3 and b_4 , in this order. Once it exits the last back child b_4 , ξ begins tracking the entering spiral for b_2 in reverse back to reach t on the front rim of b_2 , thus visiting b_3 again. From the front rim of b_2 , ξ follows b_1 's front alternating path to b_5 , then immediately to front child b_6 and then to the back of b_5 . Since b_5 has no back children, ξ reverses direction using a back face strip and begins tracking the path back to b_1 , thus visiting b_6 again. Note that ξ is moving rightwards as it reenters b_1 , therefore it proceeds to the rightmost back child b_7 of b_1 . Upon exiting b_7 , ξ moves along b_1 's back alternating path to b_8 . Note that b_8 is the last back child of b_1 to be visited, therefore the spiral segment ξ^* between

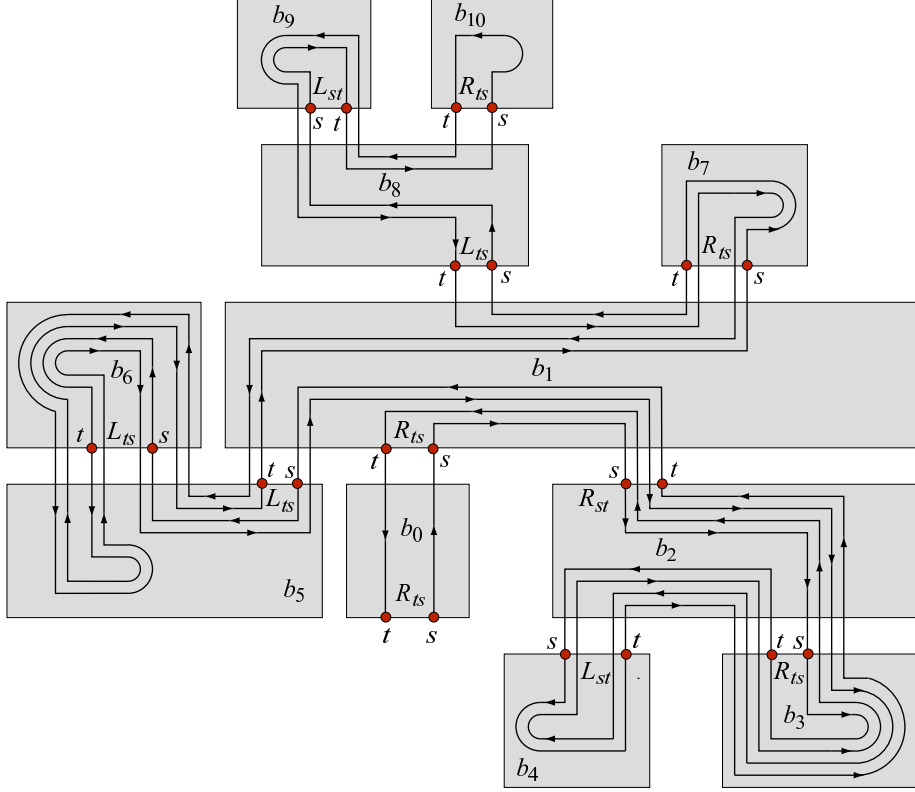


Figure 13: A complete recursive unfolding example: 2D representation.

the entering point of b_1 and the entering point of b_8 is the entering spiral of b_1 . Also note that ξ^* visited boxes in the order $b_1, b_2, b_3, b_4, b_3, b_2, b_1, b_5, b_6, b_5, b_6, b_5, b_1, b_7, b_1$, therefore the exiting spiral of b_1 will revisit the same sequence in reverse order on its way back to the front rim of b_1 . Between the entering and exiting points of b_8 , ξ visits the back children b_9 and b_{10} , then b_9 again on its way back to the front of b_8 . Fig.13 shows ξ in its entirety.

2.4 Thickening ξ

Spiral ξ established in Section 2.2.2 can be thickened in the y direction so that it entirely covers each band. This results in a vertically thicker unfolded strip. See Figure 14 for an example that illustrates the thickening procedure on the base case from Figure 3. Since the unfolded ξ is monotonic in the horizontal direction, thickening it vertically cannot result in overlap. From this point on, whenever we refer to ξ , we mean the thickened ξ .

2.5 Attaching Front and Back Faces

Finally, we “hang” the front and back faces of O from ξ in a manner similar to that done in [DFO06], as follows. Consider the set of top edges of O that separate band faces from front or back faces. These edges are each part of a rim, and hence they are found on the horizontal boundaries of the unfolded ξ as a collection of one or more contiguous segments. We partition the front and back faces of each band b by imagining the top edges on the rim of b illuminating downward lightrays in these faces. This illuminates all front and back pieces; these pieces are attached above and below ξ to the corresponding illuminating rim segments.

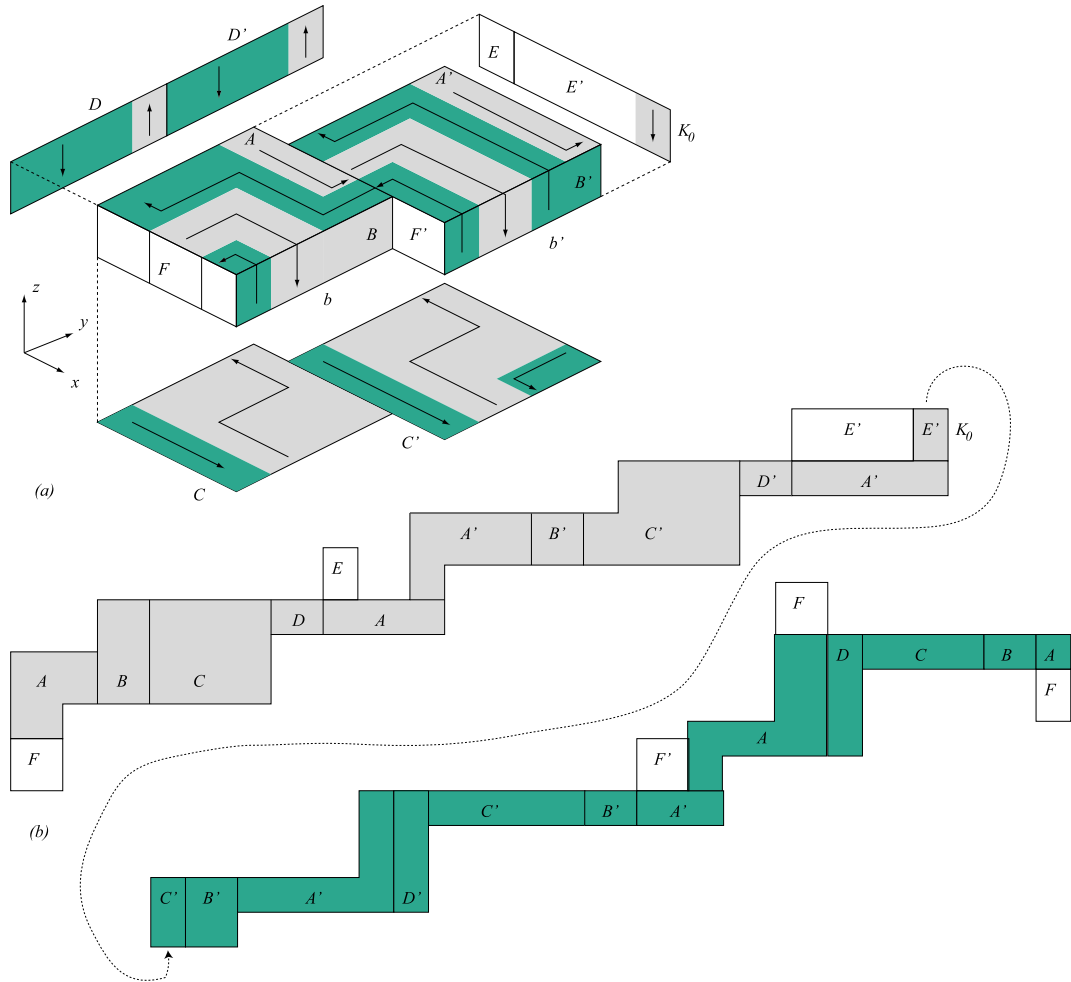


Figure 14: (a) Thickened ξ entirely covers b and b' . (b) Planar layout of spiral ξ with front and back face pieces attached above and below.

For an example, see Figure 14 showing a two band shape and its unfolding. Here the front face of band b is partitioned into three pieces which are hung from their corresponding rim segments in the unfolding. Faces E , F' and E' are hung similarly. Observe that an example of edge overlap mentioned in Section 1 occurs between face F' and a section of A in the unfolding.

This completes the unfolding process, which we summarize in the procedure $\text{UNFOLD-EXTRUSION}(O)$ below.

UNFOLD-EXTRUSION(O)

1. Partition O into bands with xz parallel planes Y_0, Y_1, \dots through each vertex (Section 1).
2. Select root band b_0 adjacent to Y_0 and compute unfolding tree T_U with root b_0 .
3. For each band b encountered in a preorder traversal of T_U
 - 3.1 $\text{LABEL-FRONT-CHILDREN}(b)$.
 - 3.2 $\text{LABEL-BACK-CHILDREN}(b)$ (Section 2.2.1).
4. Determine $\xi = \text{SPIRAL-PATH}(b_0)$ (Sections 2.1, 2.2.2).
5. Thicken ξ to cover all bands in T_U (Section 2.4).
6. Hang front and back faces off ξ (Section 2.5).

3 Unfolding All Orthogonal Polyhedra

The unfolding algorithm described for extrusions generalizes to unfolding all orthogonal polyhedra. Let O be a genus-zero orthogonal polyhedron. The surface of O is simply connected, which means that any closed curve on the surface can be continuously contracted on the surface to a point. We will use this characterization in our proofs. We start by partitioning O into bands with xz parallel planes $Y_0, Y_1, \dots, Y_i, \dots$ through each vertex.

3.1 Determining Connecting z -Beams

Define a z -beam to be a vertical rectangle on the surface of O of nonzero width connecting two band rims. In the degenerate case, a z -beam has height zero and connects two rims along a section where they coincide. We say that two bands b_1 and b_2 are z -visible if there exists a z -beam connecting an edge of b_1 to an edge of b_2 .

Lemma 2 *All z -beams between two z -visible bands lie in one Y_i plane.*

Proof: Suppose to the contrary that bands b_1 and b_2 are connected by beams in both Y_i and Y_{i+1} , i.e., both rims of both bands are connected by z -beams. Then we can construct a closed curve C on the surface of O from b_1 , following the beam on Y_i to b_2 , and following the beam on Y_{i+1} back to b_1 . See Figure 15. Now let E be a closed curve just exterior to, say b_1 , parallel to and between Y_i and Y_{i+1} . Then E and C are interlinked. This means that C cannot be contracted to a point, contradicting the genus-zero assumption. \square

Thus all the z -beams between two z -visible bands are in this sense equivalent. We select one z -beam of minimal (vertical) length to represent this equivalence class.

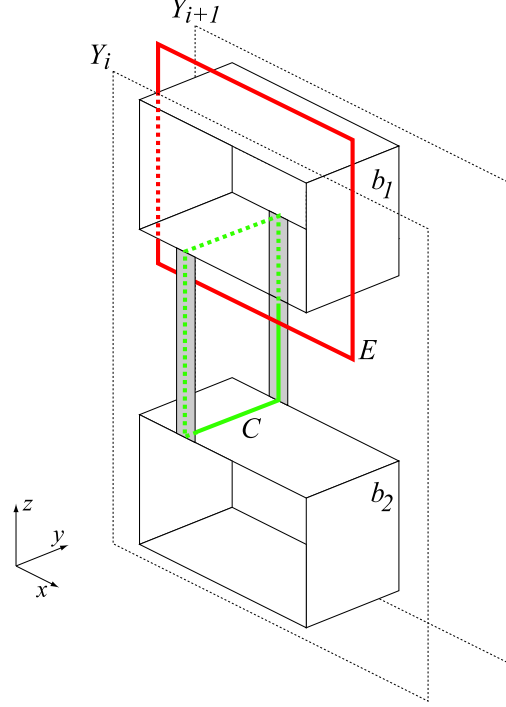


Figure 15: If two z -visible bands are connected by beams to both rims of each, then the surface curve C is interlinked with exterior curve E .

3.2 Computing Unfolding Tree T_U

Let G be the graph that contains a node for each band of O and an arc for each pair of z -visible bands. It easily follows from the connectedness of the surface of O that G is connected. Let the unfolding tree T_U be any spanning tree of G , with the root selected arbitrarily from among all bands adjacent to Y_0 .

As defined in Section 2, the rim of the root node/band at y_0 is called its *front* rim; the other is its *back* rim. For any other band b , we provide definitions equivalent to the ones in Section 2, only this time in terms of connecting z -beams: the *front* rim of b is the one to which the (representative) z -beam to its parent is attached; and the other rim of b is its *back* rim (Lemma 2 guarantees that this definition is unambiguous.) A child is a *front child* (*back child*) if its z -beam connects to the front (back) rim of its parent. We call the region of the Y -plane enclosed by a band's back rim its *back face*, and we say that the back face is *exposed* if it is a face of O .

The following lemma establishes that bands with no back children in T_U have exposed back faces. This will be important in proving the correctness of our unfolding algorithm, because we will need to employ strips from the exposed back faces to turn the spiral around, analogous to the K_0 strip in Figure 3. We note that this lemma is not true if O has a non-zero genus. Figure 16, for example, shows a polyhedron with a hole in it, whose corresponding spanning tree (depicted on the right) contains a band (b_2) with no back children and an unexposed back face.

Lemma 3 *The back face of every band in T_U with no back children is exposed.*

Proof: We begin by establishing that any two band points p and q of O are connected by a simple surface curve that follows the path in T_U between p 's band and q 's band. Let (b_1, b_2, \dots, b_k) be the path in T_U between band b_1 containing p and band b_k containing q , and let z_1, z_2, \dots, z_{k-1} be the

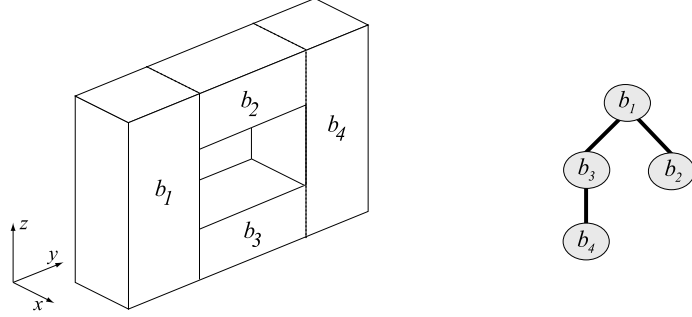


Figure 16: For this genus-1 polyhedron, the spanning tree on the right contains a band (b_2) with no back children and an unexposed back face.

z -beams connecting pairs of adjacent nodes along this path. From p , the surface curve moves to an arbitrary position on the rim of b_1 , then around the rim until it meets z_1 , then along z_1 to the rim of b_2 . In a similar manner the curve moves from b_2 to b_3 and so on, until it reaches b_k (more precisely, the line segment at the intersection between z_{k-1} and b_k). Once on b_k , the curve moves along the rim of b_k up to the point y -opposite to q , and finally in the y -direction to q . Figure 17 shows the surface curve corresponding to a five band path.

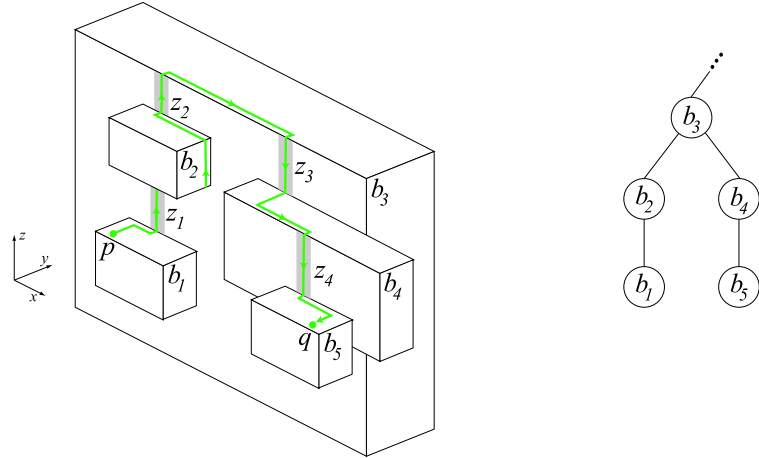


Figure 17: A surface curve corresponding to a five-band path in T_U (on the right).

Now suppose for the sake of contradiction that there is a band b with no back children whose back face is not exposed. Let r_- be the back rim of b and r_+ the front rim of b . The rim r_- connects to the surface of O , so from any point on r_- , we can shoot a vertical ray on O 's surface and it will hit another rim point, either another point on r_- or a point on some other rim. (Generally this ray will lie in a front or back face of O adjacent to r_- , but in the degenerate case when r_- coincides with another rim, the height of the ray will be zero). If the vertical rays from r_- only hit r_- again, then in fact the back face of b is exposed. So there must be some vertical ray α that extends from r_- to a point p' on some other band b' . See Figure 18.

Let p be a point on the front rim r_+ of b . We established above the existence of a particular surface curve C from p to p' corresponding to the path between b and b' in T_U . Because b has no back children in T_U , C moves from r_+ to the parent of b and never returns to b again, therefore it never touches r_- (refer to Figure 18). We now extend C to a simple closed curve that crosses r_-

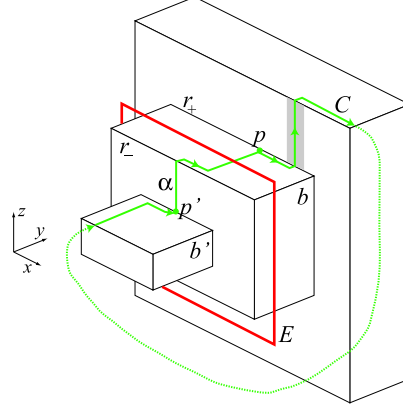


Figure 18: For a band b with no back children in T_U , an unexposed back face implies two interlinked closed curves, C on the surface of O and E exterior.

as follows: from p' , C travels along the vertical ray α to r_- , then around r_- until it reaches the point y -opposite to p , and finally it extends in the y -direction to p . Now consider a second closed curve E exterior to O that cycles around band b . Curves C and E are interlinked, meaning that C cannot be contracted to a point. This contradicts the genus-zero assumption. \square

3.3 Unfolding Algorithm

The algorithm that unfolds all bands in T_U is very similar to the algorithm that unfolds extrusions (described in Section 2). The main difference is that spiral ξ must now travel along the vertical z -beams that connect a parent to its children; these z -beams unfold vertically in the plane. The unfolding starts by assigning an entering/exiting configuration to each band in T_U (as in Section 2.2.1), then determines a spiral ξ with the properties listed in Lemma 1. Recall that ξ follows the (front, back) alternating paths on every band b in T_U , in order to reach all (front, back) children of b . Unlike for extrusions however, where an alternating path leads directly to a child b_i of b , in this case such an alternating path leads to a z -beam α connecting b_i to b ; therefore, ξ must continue along α to reach b_i .

For bands with no back children, ξ reverses direction using a strip from its back face. Lemma 3 establishes that the back faces of such bands are exposed, and hence a strip is available. Any vertical strip extending from a top to a bottom edge of the back face may be used.

Figure 19 shows a complete unfolding example, with the spiral path already thickened so that it covers the bands. The unfolding begins at point s on front box b_0 . It spirals clockwise around b_0 to the z -beam that takes it to back child b_1 . Once on b_1 , it begins following an alternating path to reach the z -beams to front children b_2 and b_3 . After spiraling around b_2 and b_3 it makes one complete cycle around b_1 and then follows the z -beam to back child b_4 . It spirals around b_4 , turns around on its back face, and then tracks back through b_4 , around b_3 , through front children b_2 and then b_1 , and finally around b_0 to point t . A small portion of the staircase-like unfolding of this example is shown in Figure 19(b).

Front and back faces of O are partitioned and attached to ξ according to the illumination model described in Section 2.5, with one modification—here both top *and* bottom edges of each rim illuminate downward lightrays. The front and back face pieces are attached to their illuminating rim segments. This is illustrated by arrows on the front faces in Figure 19. Bottom edges must illuminate light because lower bands may block rays from higher bands (which cannot occur with

extrusions). For example, bands b_0 , b_2 , and b_3 block lightrays from b_1 , but rays from their bottom edges illuminate the front face pieces below them. This method is guaranteed to illuminate all front and back faces since a ray shot upward from any front or back face point will hit a top or bottom edge of a rim before leaving the surface of O . The rim it hits is the one that illuminates it and the one to which its piece is attached.

With the exception of these changes, the algorithm remains identical to the one described in Section 2. A summary of the algorithm, with changes to the earlier procedure `UNFOLD-EXTRUSION(O)` (from Section 2) marked in italic, is provided below.

UNFOLD(O)

1. Partition O into bands with xz parallel planes Y_0, Y_1, \dots through each vertex (Section ?).
2. *Determine connecting z-beams for all pairs of z-visible bands* (Section 3.1.)
3. Select root band b_0 adjacent to Y_0 and *compute unfolding tree T_U with root b_0* (Section 3.2).
4. For each band b encountered in a preorder traversal of T_U
 - 3.1 `LABEL-FRONT-CHILDREN(b)`.
 - 3.2 `LABEL-BACK-CHILDREN(b)` (Section 2.2.1).
5. Determine $\xi = \text{SPIRAL-PATH}(\mathbf{b}_0)$ (as in Section 2.2.2, but *moving up and down z-beams*).
6. Thicken ξ to cover all bands in T_U (Section 2.4).
7. Hang front and back faces off ξ (as in Section 2.5 but illuminating light from top *and bottom rim edges*).

4 Worst Case

The thinness of the spiral path is determined by the number of parallel paths on any face, which we call the *path density* on that face. If the maximum density is k , then the path can be at most $1/k$ -th of the face width (y -extent). We say a band b_i is *visited* each time the spiral enters the band, alternates back and forth between its children, turns around using the last back child (or back face of b_i if there are no back children), and alternates between its children in reverse order, and finally exits b_i . If there are m parallel paths on a face after the first visit, then after v visits there are vm parallel paths, since each subsequent visit tracks alongside a path laid down during an earlier visit. For example, Figures 3–5 show a single box visited once, and there are 4 parallel paths on the top face: two from s to turnaround, and two back to t . Figure 12 shows that with the exception of the turnaround box (b_{10} in this example) boxes at depth $d = 1$ ($b_1 - b_9$) are visited twice, doubling their path densities to $8 = 2 \times 4$.

We now use this doubling property to construct an example that has path density $2^{\Omega(n)}$, where n is the number of vertices of the polyhedron. We use a skewed binary tree, as illustrated by the sequence of extrusions (viewed from above) in Figures 20a-c. In each case, the spiral starts on the bottom box heading to the right. Each non-leaf box has two back children; the right child is visited first and the left one is the turnaround box. The number of times each leaf box is visited is marked. One of the children at depth d (shaded in the figure) is visited 2^d times and has a path density of $2^d 4$. A depth- d tree of this structure contains $2d + 1$ boxes total, and so can be realized by a polyhedron with $n = 8(2d + 1)$ vertices. Thus $d = \Omega(n)$, and the shaded child has a path density of

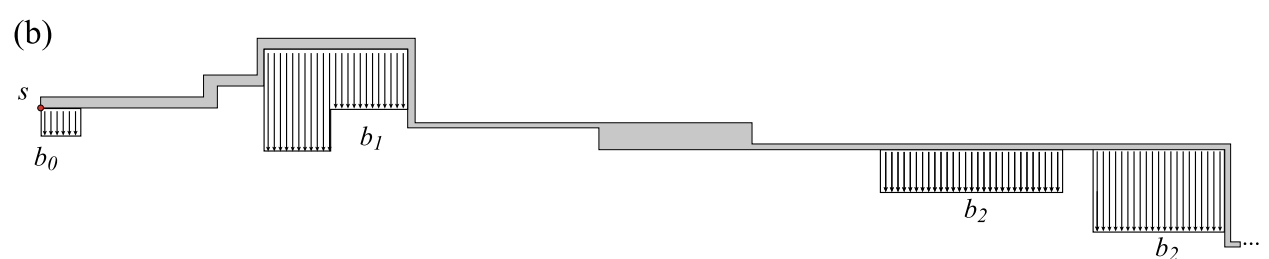
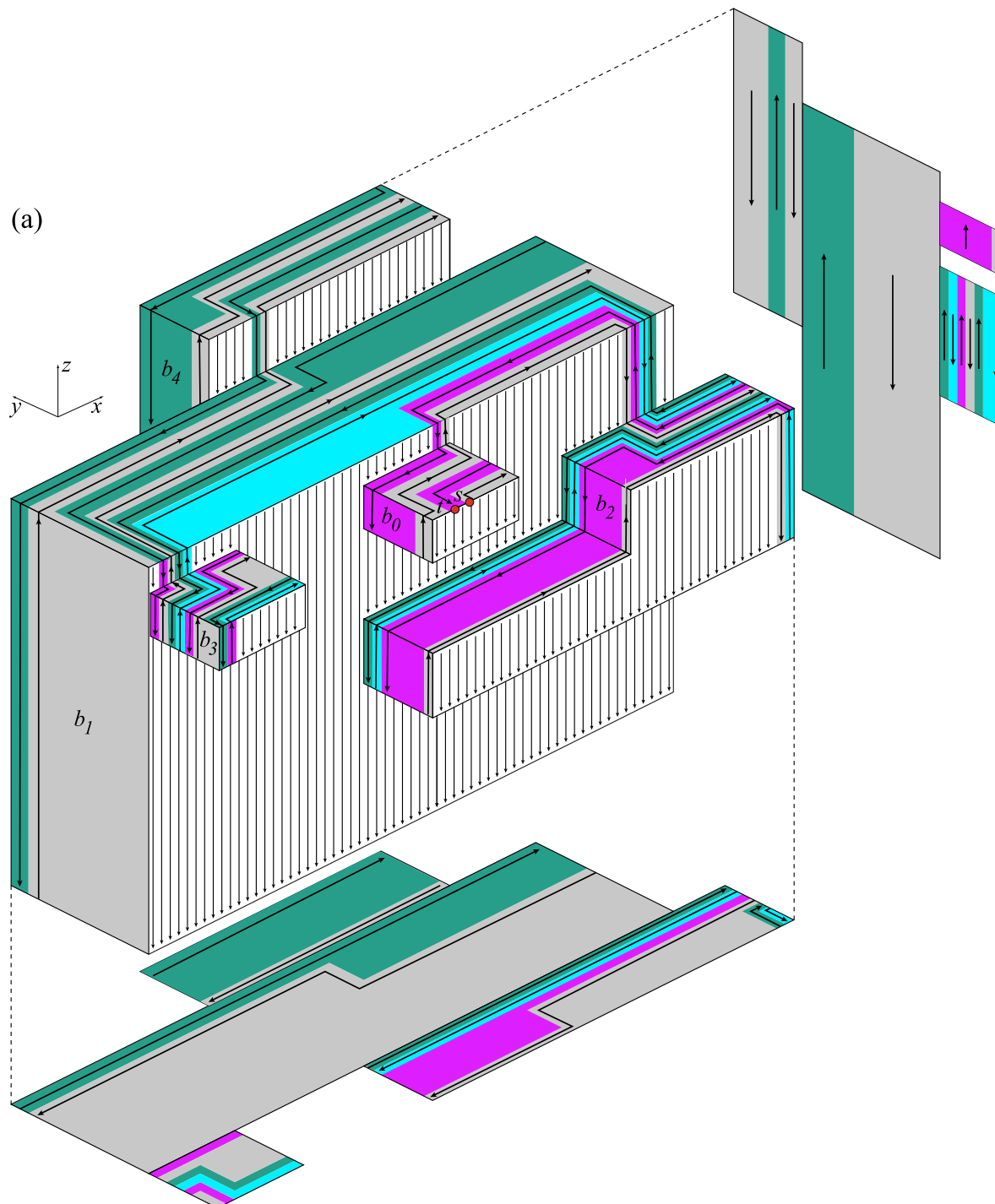


Figure 19: (a) Four-block example; (b) Prefix $21f$ unfolding (not to same scale), with front face pieces labeled.

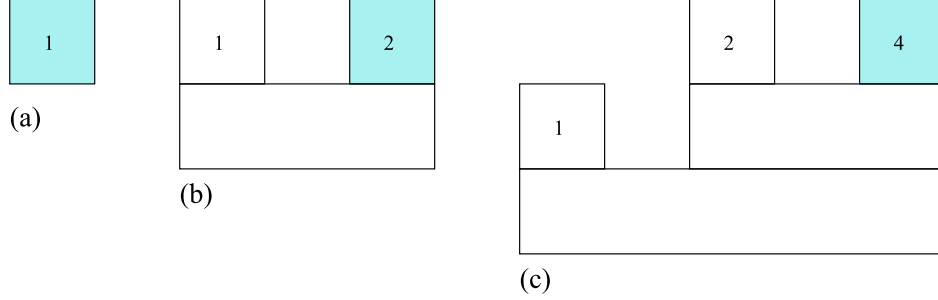


Figure 20: One back child has path density $2^d 4$.

$2^{\Omega(n)}$. We conclude that the spiral path may need to be as thin as $\epsilon = 1/2^{\Omega(n)}$ times the smallest y -extent of any face of the polyhedron.

We now establish a density upper bound of $2^{O(n)}$. Observe that each time a band is visited, its children are visited at most twice, and therefore 2^d is an upper bound on the number of visits for a band at depth d . It can be that the most dense band is not a leaf, but a band having many children. As Figure 11 makes clear, the number of parallel paths, m , laid out on each visit depends on the number of children a band has, due to the alternation back and forth to each child. Noting that both m and d are $O(n)$, we can conclude that the path density is bounded by $m2^d = O(n)2^{O(n)}$, which is still $2^{O(n)}$.

Theorem 4 *The path density from the described algorithm is $2^{\Theta(n)}$, and so $\epsilon = 1/2^{\Theta(n)}$, in the worst case.*

5 Conclusion

We feel it is feasible to extend our algorithm to handle orthogonal polyhedra with genus ≥ 1 . One idea is to treat holes as being blocked by virtual membranes, and to unfold according to our genus-0 algorithm, and then compensate for the virtual faces. However, a number of details in such an algorithm would need careful handling.

An extension that seems beyond reach of our current techniques is to achieve a $k \times k$ refined grid unfolding, for k a constant, independent of the number of vertices n of the polyhedron. Our algorithm fundamentally relies on ϵ -thin strips.

Finally, it our spiraling technique so relies on the orthogonal structure of the polyhedra that it seems difficult to use it to help resolve the open problem of whether every polyhedron may be unfolded.

References

- [BDD⁺98] T. Biedl, E. Demaine, M. Demaine, A. Lubiw, J. O'Rourke, M. Overmars, S. Robbins, and S. Whitesides. Unfolding some classes of orthogonal polyhedra. In *Proc. 10th Canad. Conf. Comput. Geom.*, pages 70–71, 1998.
- [DEE⁺03] E. D. Demaine, D. Eppstein, J. Erickson, G. W. Hart, and J. O'Rourke. Vertex-unfoldings of simplicial manifolds. In Andras Bezdek, editor, *Discrete Geometry*, pages 215–228. Marcel Dekker, 2003. Preliminary version appeared in *18th ACM Symposium on Computational Geometry*, Barcelona, June 2002, pp. 237–243.

- [DFO05] Mirela Damian, Robin Flatland, and Joseph O'Rourke. Unfolding Manhattan towers. In *Proc. 17th Canad. Conf. Comput. Geom.*, pages 204–207, 2005.
- [DFO06] Mirela Damian, Robin Flatland, and Joseph O'Rourke. Grid vertex-unfolding orthogonal polyhedra. In *Proc. 23rd Sympos. Theoret. Aspects Comput. Sci.*, Lecture Notes Comput. Sci. Springer-Verlag, 2006. To appear.
- [DIL04] E. D. Demaine, J. Iacono, and S. Langerman. Grid vertex-unfolding of orthostacks. In *Proc. Japan Conf. Discrete Comp. Geom.*, November 2004. To appear in LNCS, 2005.
- [DO04] E. D. Demaine and J. O'Rourke. Open problems from CCCG 2004. In *Proc. 16th Canad. Conf. Comput. Geom.*, 2004.
- [DO05] E. D. Demaine and J. O'Rourke. A survey of folding and unfolding in computational geometry. In J. E. Goodman, J. Pach, and E. Welzl, editors, *Combinatorial and Computational Geometry*. Cambridge University Press, 2005.